Quest Journals
Journal of Architecture and Civil Engineering
Volume 3 ~ Issue 6 (2017) pp: 01-11
ISSN(Online) : 2321-8193
www.questjournals.org

Research Paper

Dynamic Response of Three Historic Through-Truss Bridges

[1]Brandon Newpher,[2*]Jeffrey A. Laman, PhD, PE,
[3]Thomas E. Boothby, PhD, PE, RA

[1]Bridge Engineer McCormick Taylor, Engineers and Planners 7 Parkway Center, Suite 700 Pittsburgh, United States of America
[2]Professor of Civil Engineering The Pennsylvania State University Department of Civil and Environmental Engineering 231J Sackett Building University Park, United States of America
[3]Professor of Architectural Engineering The Pennsylvania State University Department of Architectural EngineeringUniversity Park, United States of America
Corresponding Author: Jeffrey A. Laman, PhD, PE

Received 25 September, 2017; **A**ccepted 10 October, 2017 © The Author(S) 2017. **P**ublished with openaccess at **Www.Questjournals.Org**

ABSTRACT: *The late 1800s was a time of significant innovation in bridge engineering resulting in the construction of many unique bridge forms. These bridges, now well beyond their design life, are being evaluated for capacity, leaving many to be demolished, while few are being rehabilitated. To evaluate the adequacy of a historic, through-truss bridge requires the evaluation of complex dynamic behaviour under traffic loading. Historically, this complex dynamic behaviour is condensed into a single dynamic load factor (DLF), enabling the enveloping of dynamic response magnitude by scaling the static design response. The present study objective is to evaluate the magnitude, the distribution, and the influential variables affecting DLF for historic through-truss bridges. This was accomplished through a combination of field evaluation of existing specimens, digital signal processing, and data comparison to evaluate DLF magnitude, distribution, and correlations with test variables. Correlations and trends were investigated between DLF magnitude and: maximum static strain, vehicle speed, vehicle static weight, and bridge span. The most influential variable affecting the magnitude of DLF was determined to be member peak static strain. The current study concludes that historic through-truss bridges exhibit DLFs with magnitudes higher than contemporary slab on girder bridge types.*

Keywords: Bridge, Truss, Dynamic, Impact, Historic

I. INTRODUCTION

The late 1800s was a time of significant innovation in bridge engineering. During this period, through-truss bridges of many designs became common constructed structural forms in the North-Eastern United States. Historic bridges have unique and aesthetically pleasing features that are rarely exhibited in their modern counterparts. A century of floods and deterioration have left only a select few of these historic bridges to remind us of these once prominent structural forms. The renewed focus on the state of deteriorated infrastructure, in conjunction with the age and deterioration of historic truss bridges, has served to increase the risk of a historic bridge being found structurally deficient, demolished, and replaced resulting in a great loss of structural and architectural history.

A primary factor in determining the fate of a historic bridge lies in the treatment and understanding of their complex dynamic behaviour when exposed to contemporary traffic loading. The most commonly used technique in practice for dealing with complex dynamic loading is the application of a dynamic load factor (*DLF*) as defined by Equation 1 in which R_{dyn} and R_{static} correspond to the dynamic and static response magnitudes respectively. This technique accounts for bridge dynamics by scaling the static response magnitude to envelope the relatively higher dynamic response. Bridge components are then designed or evaluated for this effective static load, removing the need for a detailed dynamic analysis. Standard magnitudes of the DLF exist in all major bridge design codes, but have been developed primarily for use with modern bridge forms. Historic truss bridges having a relatively lower mass to stiffness ratio are likely to exhibit different dynamic behaviour than the modern girder bridges that were studied to create the existing DLFs.

(1)

Previous studies (Laman 1999, Paultre 1992) have not provided a widely accepted *DLF* for the evaluation of through-truss bridges; leaving only extensions of results based on contemporary structural forms. These studies have established competing methods to produce DLFs that can be categorized as either analytical or experimental. It has been shown (Deng 2010, Hwang 1991, Moghimi 2008) that analytical finite element models can be used to predict *DLF* but simulations rely heavily on assumptions or detailed model validation via measured response. It has also been shown (Ashebo 2007, Billing 1984, Kim 1997, Nowak 1998, Obrien 2009, OConnor 1985) that several field measurement methods can be used to determine *DLF*s. The first method involves driving a test vehicle over an existing bridge at crawl and several speed levels to directly measure the static and dynamic strain responses. This approach, however, introduces error as a result of inconsistent test vehicle travel paths in each test as well as the inherent variability of field testing. Alternately, measured *DLF*s can be obtained through the field measurement of dynamic response and the implementation of digital filtering to extract corresponding static response quantities. This eliminates the errors associated with using multiple test vehicle runs to measure strains and therefore the *DLF* and is the method employed in the present study.

The current study determines *DLF*s through Equation 1 by collecting field measurement of dynamic strains in conjunction with a digital filter to obtain static response. This approach allows the determination of *DLF*s under normal traffic conditions and vehicles. *DLF*s for three historic through truss bridges under controlled truck and normal traffic conditions were obtained in this manner. Instrumentation was placed on up to sixteen bridge truss members to allow recording of strain-time histories under controlled and random vehicle traffic. In addition, a variable frequency dynamic shaker was used to excite the bridge to facilitate the identification of natural frequencies for each bridge.

To determine the parameters that most significantly affect the *DLF* magnitude, the following test parameters were controlled or documented for each test case:

- bridge length;
- vehicle speed; and
- vehicle static weight (controlled testing only).

Gaining a better understanding of the complex relationship that exists between bridge loading and dynamic response is especially important when evaluating the adequacy of historic structures. Maintaining the simplicity of the *DLF* while increasing the accuracy could reduce the cost of accurate analysis of historic truss bridges and therefore aid in preservation efforts.

II. STUDY DESIGN

The study of historic bridge *DLF*s relies on the development of a logical process to obtain the dynamic and static response of the bridge during the passage of truck traffic. For the present study the responses were obtained using a two-step process: 1) field data was recorded including: vehicle presence, vehicle speed, member strains due to traffic events, and member strains due to a generated forcing function; and 2) dynamic strain time-histories were filtered for all frequencies other than the static component to separate the dynamic and the static responses.

The most important data required to complete the present study are member strain time-histories caused by traffic events. To collect this dynamic strain data, a data acquisition system was configured and connected to linear variable displacement transducers (LVDTs) installed to capture the bridge member elongation over a known length. When selecting the members and locations to install LVDTs, practical limitations and signal to noise ratio were considered. To maximize the signal to noise ratio, members and sensor placement were selected on the basis of the highest dynamic strains. In all bridges the members closest to the loading were expected to exhibit high dynamic strains, therefore stringers and floor beams were instrumented at mid-span. For truss members that respond primarily with high axial forces, sensors were placed according to accessibility and in locations so as to avoid stress concentrations at connections.

Vehicle presence and speed was determined with four tape switches placed on the roadway in the wheel path at known spacing and distance from the bridge bearing. By placing two tape switches at each end of the known bridge length vehicle presence and average speed was determined. This information is vital in determining the time range of the data of interest and the static loading frequency.Analog signals were digitized using a Daqbook 216 A/D converter; determining the correct sampling rate for this process is a key decision in the testing procedure. For the purpose of the present study the frequencies of interest were the natural frequencies of the bridge and bridge components. Preliminary calculations of member local natural frequencies for stiffer members such as bridge stringers and floor beams fell in the range of 20 Hz to 40 Hz. Considering this range of interest and the need to ensure accurate maximum values in the data, a sampling rate of 200 Hz was selected, which corresponds to more than two times the Nyquist rate.

Because the selected historic bridges are located on low volume traffic routes, controlled testing consisted of passing a known weight test vehicle at known speed over the bridge. The weight of the test vehicle was a concern in vehicle selection as a vehicle at or near the weight limit of the bridge was utilized. This limitation resulted in two test vehicles: a standard, single axle dump truck for low weight limit bridges; and a water tanker for higher weight limit bridges. Test vehicle speeds were incremented starting with 5 mph (8 km/h) increasing by 5 mph (8 km/h) until the speed limit, maximum attainable, or safe test vehicle speed was reached.

Modal testing was conducted for each selected bridge to aid in the identification of natural frequencies which are vital to the determination of filter cut-off frequencies. Modal testing consisted of exciting the bridge with a known forcing function while taking strain measurements. A frequency response function (FRF) was then created to identify the natural frequencies of each bridge and instrumented bridge member. A long stroke electromagnetic shaker was used to produce known frequency, force-time histories in the range of 40 to 45 kg. The shaker was placed on the bridge deck at mid-span and used to excite the bridge in a vertical motion, simulating the primary direction of traffic loading. An accelerometer was attached to the shaker to validate the forcing function supplied to the bridge and aid in the FRF calculation.

The three historic bridges selected for field-testing are described in Table 1. The primary bridge selection parameters were: 1) the original construction date; and 2) open to vehicular traffic. Bridges 1 and 3 were recently rehabilitated and are open to truck traffic, while bridge 2 is in original condition with only the floor system having been replaced. Sensors were installed on critical members of the truss and floor system including: top chord, bottom chord, diagonals, stringers and floor-beams.

Table 1: Selected Bridges for Testing

No.	Name	Location	Bridge Type	Span	Year Built
1	Pine Creek	Jersey Shore, PA	Lenticular Arch	88.4 m	1889
2	Old Forge	Camp Hill, PA	Pratt Truss	34.7 m	1887
3	Neff	Alexandria, PA	Pratt Truss	46.6 m	1889

The bridge 1 test vehicle is a 3-axle, 2,500 gallon water tanker weighing approximately 21 tons (209 kN). Controlled testing consisted of 5 passes of the test truck. The testing commenced with a 5 mph (8 km/h) pass and each successive pass the speed was increased by 5 mph (8 km/h) to a maximum of 25 mph (40.2 km/h). During testing it was observed that the largest deflections in the bridge occurred during the 20 mph (32 km/h) test run. Forty-five other vehicles, both trucks and passenger vehicles, were observed during normal traffic testing.The bridge 2 test vehicle is a 2-axle dump truck weighing approximately 5 tons (50 kN). Controlled testing consisted of 10 passes beginning with a 5 mph (8 km/h) pass. Every two passes the speed was increased by 5 mph (8 km/h) to a maximum of 25 mph (40 km/h). During testing it was observed that the largest deflections in the bridge occurred during the 25 mph (40 km/h) test run. 40 other vehicles were observed during normal traffic testing.The bridge 3 test vehicle was a 3-axle fire engine, weighing approximately 23 tons (229 kN). Controlled testing consisted of 9 passes beginning with a 5 mph (8 km/h) test. Every two passes the speed was increased by 5 mph (8 km/h) to a maximum 30 mph (48 km/h). During testing it was observed that the largest deflections in the bridge occurred during the 25 mph (40 km/h) test. 33 other vehicles were observed during normal traffic testing.

After field-testing of all three bridges was completed, the LVDT displacement data was processed to compute the DLFs for each strain time-history. The dynamic response was obtained through low pass digital filtering to remove high frequency noise. The resulting dynamic response was then further filtered to obtain the static response component. The primary concern was the proper selection of both cut-off frequencies. Theoretical static frequency, static influence lines, frequency response functions from modal testing, and theoretical modal frequencies were evaluated to assist in the selection. After appropriate cut-off frequencies were determined, the static and dynamic response for each vehicle pass was determined using a fourth order Butterworth filter. Finally the maximum response values from both the static and dynamic responses were identified and input to equation 1 to calculate a *DLF* for each pass.

III. RESULTS AND COMPARATIVE STUDY

An evaluation of the *DLF* data was conducted to examine both the magnitude range of the observed *DLF*s and relationships between the magnitude and bridge and vehicle parameters. Graphs of the *DLF* data as a function of the parameter of interest were observed and correlations between *DLF* and the several parameters were evaluated.A total of 419 *DLF*s were calculated with a maximum magnitude of 1.95, 50th percentile of 1.19, and 95th percentile of 1.49. Figure 1 presents the *DLF* magnitude frequency distribution of all three bridge tests. The histogram interval was chosen to limit the number of ranges such that 4 or more data points were included. It was observed that this distribution resembles a positively skewed distribution. Comparison of experimentally derived data to the 1.33 design DLF specified by the AASHTO LRFD Bridge Design Specifications indicates that 82% of the observed DLFs fall below AASHTO.

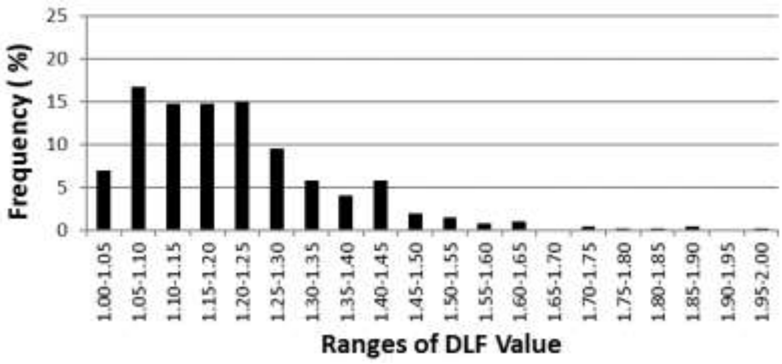

Figure 1: Histogram of DLF Magnitude Distribution (419 Samples)

The *DLF*s presented in Figure 1 include a wide mix of bridge members: truss chords, portal members, floor beams, stringers, and truss diagonals at a loading/GVW level what might be required for design or evaluation/rating. Figure 2a) presents the *DLF*s for the top chord, bottom chord, portal and diagonal members of Bridge 2 and Bridge 3 obtained from the test vehicle passes only. High levels of noise combined with low strain levels necessitated the exclusion of data from Bridge 1. The two bridges included were loaded at or above their respective weight limits during controlled testing and, therefore, *DLF*s resulting from these passes correspond closely to bridge service level loading. To further eliminate low level loading from the data, static strain level limits of 50 and 100 micro-strain were applied. The distributions corresponding to the limited static strain samples are presented in Figures 2b) and 2c). Separate graphs illustrate that the positively skewed distribution is evident in all of the samples but is most pronounced in the higher static strain level data. This clearly indicates that high *DLF* magnitude corresponds to low levels of loading/GVW that are not of interest during design or evaluation/rating. For this reason the values for *DLF* determined by the distributions corresponding to high level loading should be used for the evaluation of historic through truss bridges.

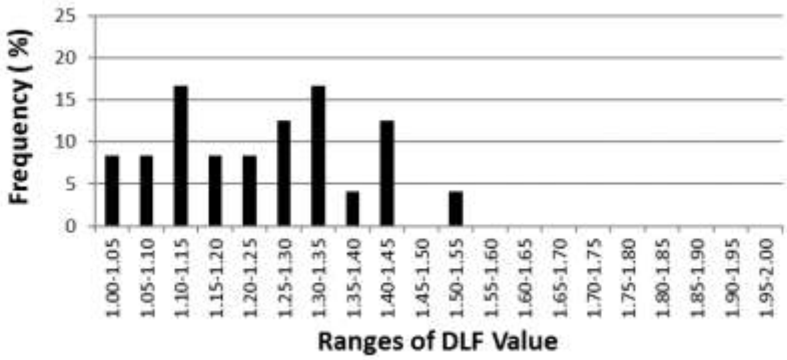

a) All Controlled Test Vehicle Passes (65 data)

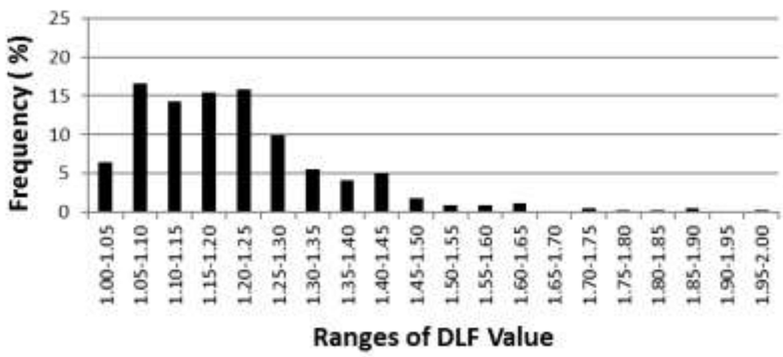

b) Maximum Static Strain Greater than 50 Micro-Strain (40 data)

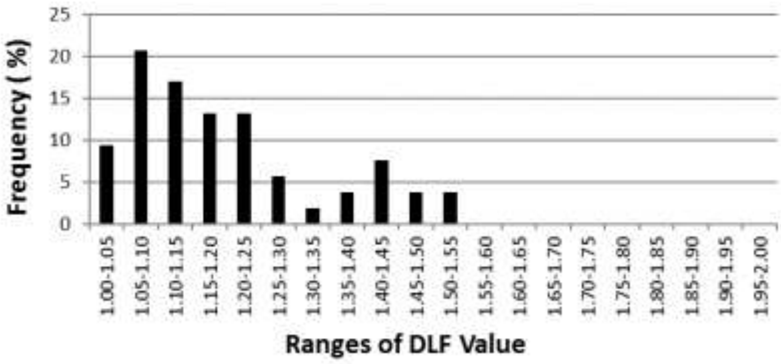

c) Maximum Static Strain Greater than 100 Micro-Strain (21 data)

Figure 2: DLF Magnitude Distribution for Global Members at Service Level Loading

Table 2 compares the DLF distributions from the observed service level loading to the corresponding AASHTO code value of 1.33 including: data size, 95th percentile, AASHTO specified DLF, and the percent of the observed distributions that fall below the AASHTO code value of 1.33. Examining the data in this way demonstrates that the 95th percentile is above the AASHTO 1.33, however, as static strain increases, the 95th percentile *DLF* magnitude decreases and the percent below 1.33 increases. Additional testing to increase data size and static strain levels will strengthen this observation, however, it can reasonably be concluded that the historic through-truss bridges tested responded with *DLF*s slightly higher than those suggested by the current AASHTO specifications when loaded at or near the current weight limits.

Table 2: Comparison of Test Vehicle *DLF* to AASHTO

Micro-strain	Data Size	95th Percentile	AASHTO	AASHTO %
0	65	1.49	1.33	74
50	40	1.40	1.33	90
100	21	1.36	1.33	91

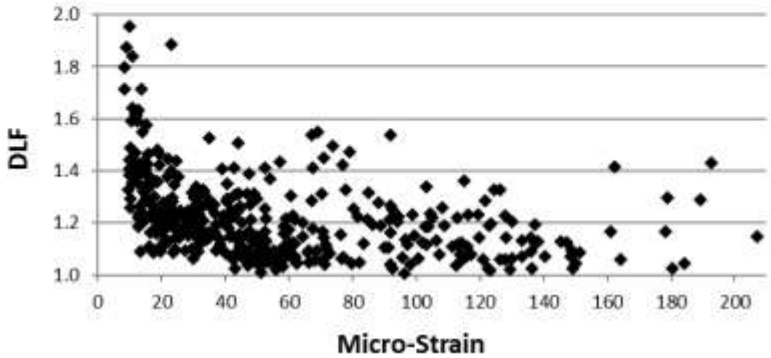

Figure 3: *DLF* versus Maximum Static Strain (All Data)

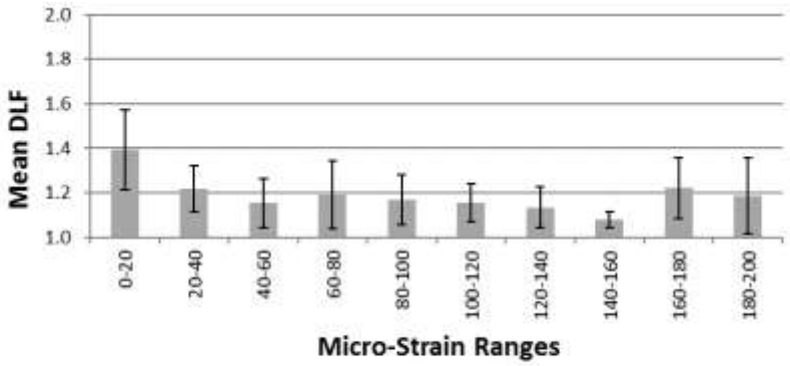

Figure 4: Histogram of *DLF* versus Max Static Strain (All Data)

Figure 3 also presents the broader relationship between maximum static strain and *DLF* magnitude, including all bridges at all load levels. An observable, general decrease in the magnitude of *DLF* as the maximum
static strain increases is supported by a Pearson's correlation coefficient of - 0.37. To further investigate this negative correlation, Figure 4 was created to condense and clarify the information presented in Figure 3. The average *DLF* magnitudes are shown for each range of maximum static stress with one standard deviation error bars. This histogram establishes a clearly observable negative correlation between the maximum static strain and *DLF* magnitude. The increase in *DLF* and variability in the 160 to 200 micro-strain range can be attributed to the small number of data points (10) in this strain range caused by a single vehicle crossing. Figure 5 presents *DLF* results for each of the three bridges. It can be observed that the trend of decreasing *DLF* with increasing static strain remains; however, there are clear differences between the responses of the bridges to vehicle traffic. The larger, Bridge 2 data set presents this trend with the highest confidence;however, the Bridge 1 and Bridge 3

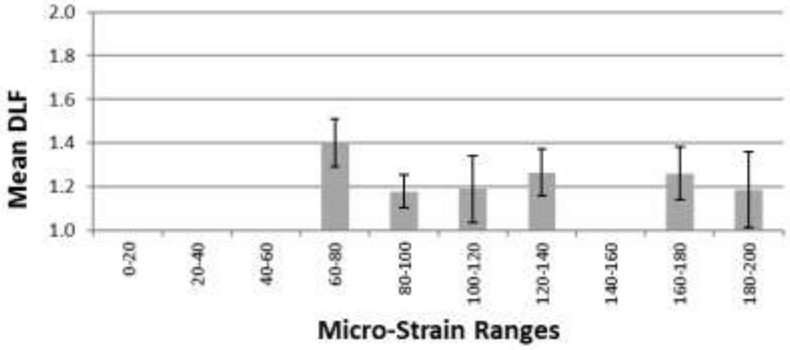

a) Bridge 1, Mean *DLF* vs Micro-Strain

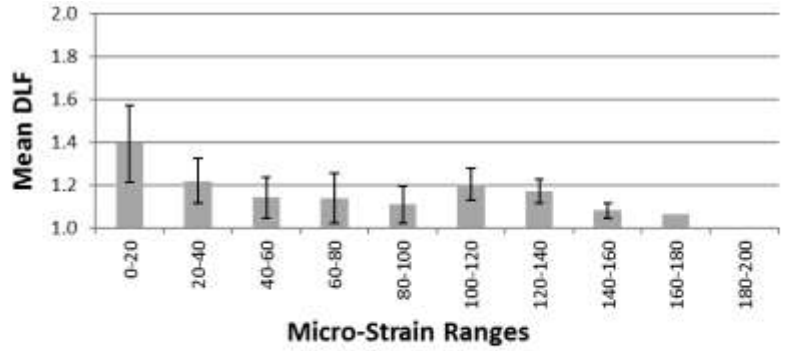

b) Bridge 2, Mean *DLF* vs Micro-Strain

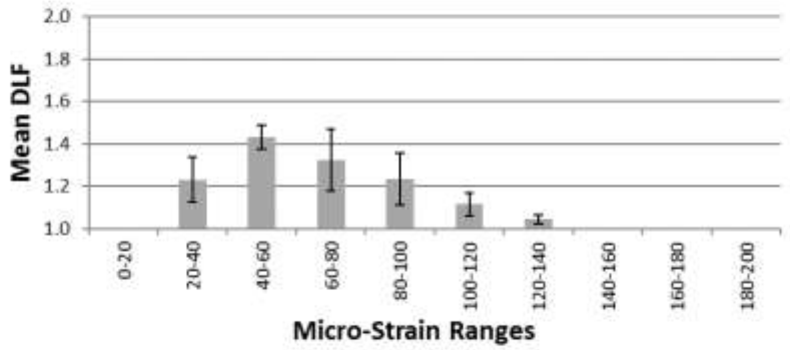

c) Bridge 3, Mean *DLF* vs Micro-Strain

Figure 5: Histograms of Mean *DLF* vs. Maximum Static Micro-Strain

smaller data sets also exhibit the trend. This observation is important because it is recognized that the large static strain scaled by the lower *DLF* results in higher design/evaluation strain (or stress) than the small static strain scaled by the higher *DLF*. Therefore, all *DLF*s are not of equal interest and it is reasonable to exclude from consideration most of the very high *DLF* magnitudes as they are not relevant for design or rating evaluations.

To further investigate *DLF*s derived from higher level loading, *DLF*s obtained for Bridge 2 and Bridge 3 members affected by vehicle load regardless of load position on the bridge (referred to here as primary members) under controlled traffic testing are plotted as a function of maximum static strain presented in Figures 6 and 7. These *DLF* magnitudes derived from the test vehicles more closely correspond to service level loading but it can be seen that low maximum static strain is still present in the data because not all instrumented members experienced large strains as a result of large GVW vehicles. The overall observed trend when all of the *DLF* data is included is further supported by Figures 6 and 7 as higher levels of static strain correspond to a much lower *DLF*. The *DLF* vs. micro-strain data presented in Figure 6 correlates at - 0.50, demonstrating a stronger relationship than when low-level loading is included.

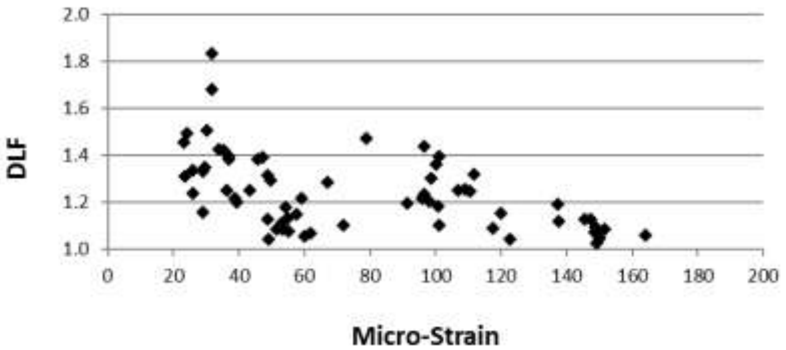

Figure 6: DLF for Primary Members at Service Loading versus Maximum Static Strain

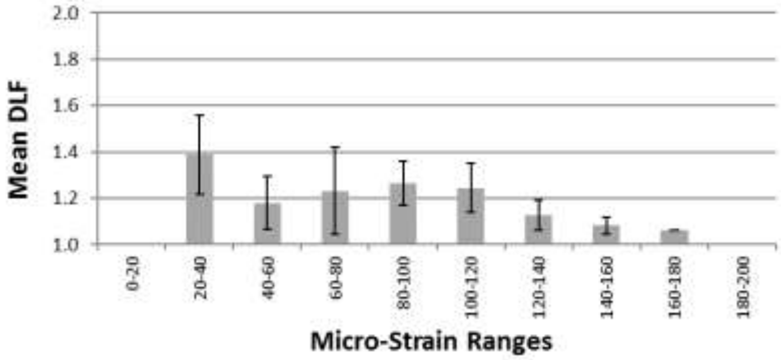

Figure 7: Histogram of *DLF* for Primary Members at Service Load vs Max Static Strain

The strength of the relationship between vehicle speed and *DLF* magnitude was investigated by plotting *DLF* as a function of vehicle speed and is presented in Figure 8. From Figure 8 it is not readily apparent that a relationship between speed and DLF exists. The computed correlation coefficient between *DLF* and speed is 0.004 suggesting no relationship. However, when the data is presented as mean *DLF* vs speed histogram of Figure 9, an observation can be made – it appears that the intermediate speeds (10 to 15, 15 to 20, and 20 to 25) result in higher *DLF* magnitudes. The Figure 10 histograms of mean *DLF* vs. speed for individual bridges also supports this observation. This relationship is the result of frequency matching between the vehicle period and/or vehicle dynamics and the natural bridge modes. More detailed testing, including an investigation of vehicle suspension characteristics would be required to investigate this hypothesis.

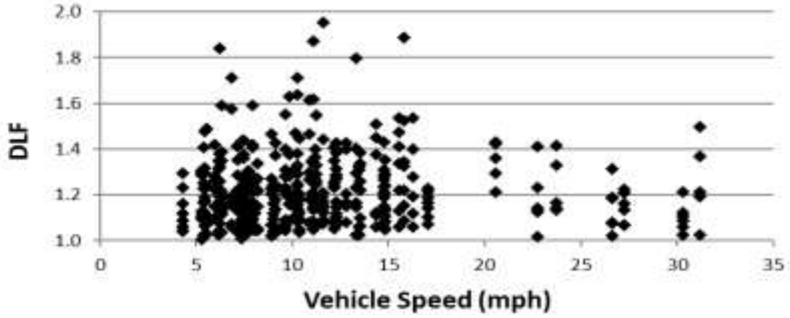

Figure 8: *DLF* versus Vehicle Speed (All Samples)

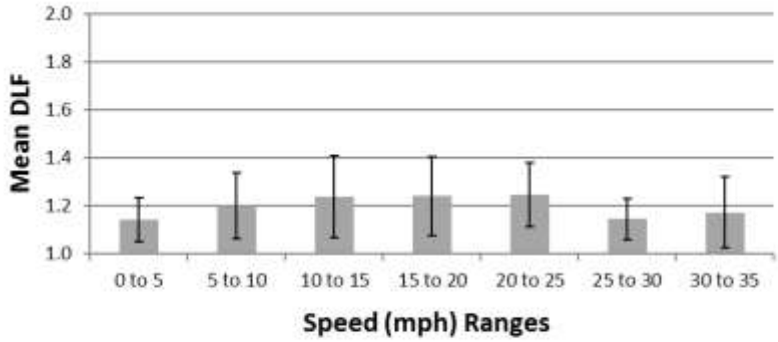

Figure 9: Histogram of *DLF* versus Vehicle Speed (All Samples)

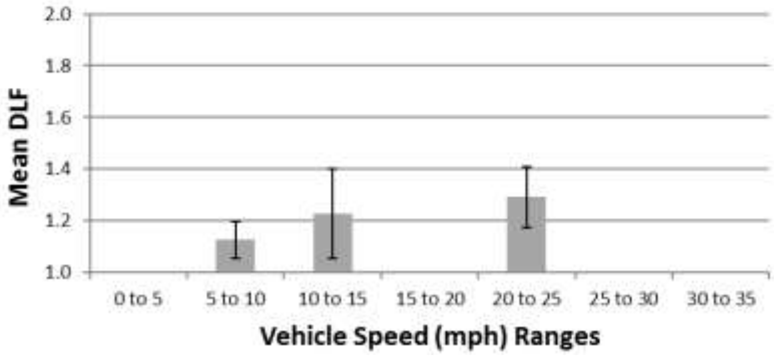

a) Bridge 1 Mean *DLF* vs Vehicle Speed

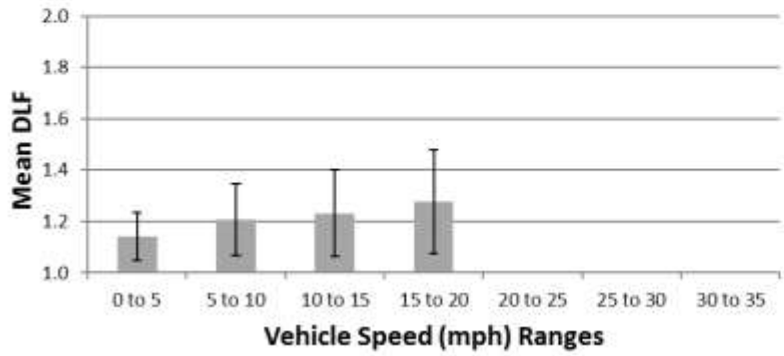

b) Bridge 2 Mean *DLF* vs Vehicle Speed

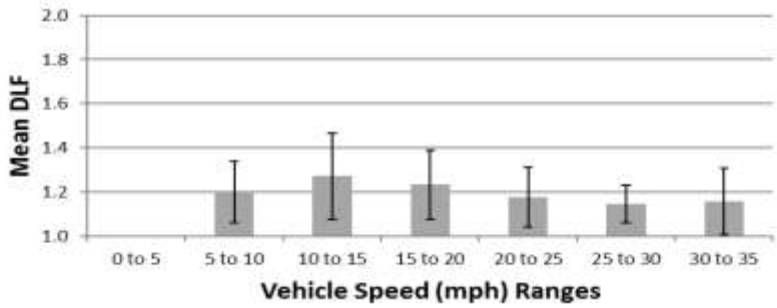

c) Bridge 3 Mean *DLF* vs Vehicle Speed

Figure 10: Histogram of Mean *DLF* versus Vehicle Speed

An investigation of the relationship between GVW and *DLF* magnitude is limited due to the very limited number of vehicles of known weight -- control test vehicles weighing 5, 10, 42 and 46 kips (22, 44, 187, and 205kN). An observation of the data presented in Figure 11 indicates that more data is required for any conclusion to be drawn.

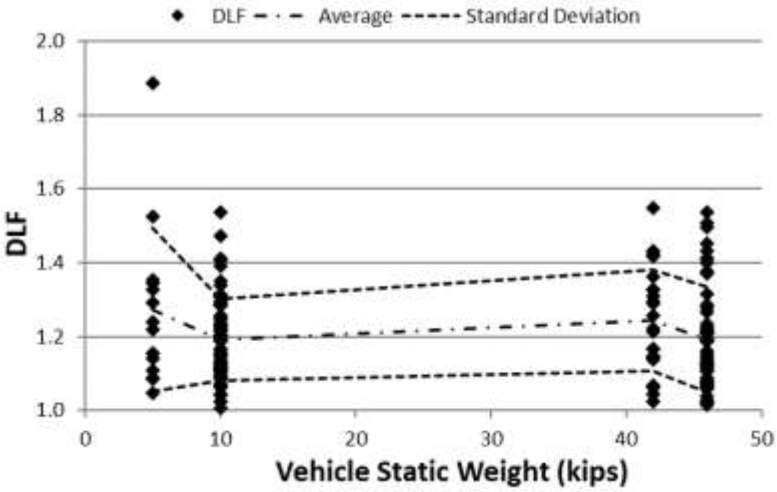

Figure 11: *DLF* versus Test Vehicle GVW

DLF magnitude as a function of bridge length was also evaluated and is presented in Figure 12. This graph illustrates that the shortest bridge responded with both the largest *DLF* magnitudes and the largest variability. The converse can also be observed – that both *DLF* variability and magnitude decreased with increasing bridge length. The histogram of Figure 12 exposes a trend of *DLF* magnitude decreasing as bridge length increases. Assuming a fixed span to depth ratio, the material volume required to construct a bridge increases exponentially as it gets longer and, therefore, the bridge dead weight significantly increases, directly affecting the bridge dynamic response. The effect of the excitation a vehicle imposes on the bridge/vehicle system diminishes as the mass of the bridge becomes much larger than the mass of the vehicle -- long bridges are more massive and less affected by relatively small mass excitations. The shortest bridge in the present study is significantly lower mass and two longer bridges are of comparable larger mass due to the medium length bridge having a concrete deck and the long span having an open grate deck. Therefore, the differences in deck type counteracted the length effects and produced *DLF*s of similar magnitude and distribution for the second two bridges.

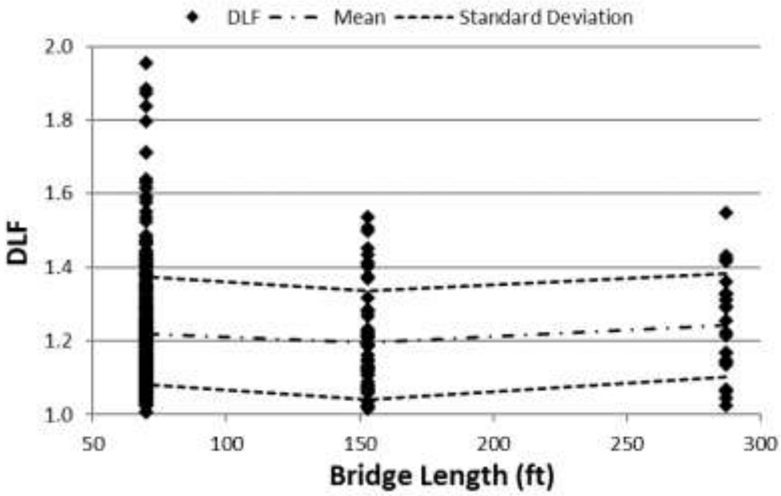

Figure 12: *DLF* versus Bridge Length – All Data

Table 4 presents the *DLF* data 95th percentile for each bridge and the corresponding length dependent, code-based *DLF*-- AASHTO*Bridge Design Specifications* (1992), *Specifications for Highway Bridges* (Japan Road Assoc., 2014), *Bridge Design*, France, and Merriman and Jacoby (1909) as presented in Table 3.

Table 3: Length Dependent *DLF* (Moghimi 2007)

Specification	*DLF*
AASHTO 1992	$DLF=1+\frac{50}{L(ft)+125}\leq 1.3$
Japan	$DLF=1+\frac{6.1}{L(\text{ft})+15.2}$
French	$DLF=1+\frac{1.2}{L(\text{ft})+1.5}$
Merriman and Jacoby	$DLF=1+\frac{300}{L(\text{ft})+300}$

The 95th percentile *DLF* exceeds all specification *DLF*s but is less than Merriman and Jacoby. This difference is attributed to the different bridge types and different live load model prescribed for each specification. Modern specifications expect a slab-on-girder bridge with significant magnitude design live load. Merriam and Jacoby is based on a through-truss bridge with heavy railcars as the design load model. The Merriam and Jacoby presumed bridge conditions more closely resemble the tested bridge live to dead load ratio of the present study, where live load on the bridge represents a significant proportion of the total system mass. In contrast, slab-on-girder bridge mass, or self-weight, is generally a higher portion of the total system mass, therefore responding to a lower *DLF* magnitude.

Table 4: Comparison of *DLF* Magnitudes to Bridge Length Varying Codified Values

Bridge #	Observed 95th	AASHTO 1992	Japan	France	Merriman and Jacoby
2	1.49	1.21	1.24	1.10	1.72
3	1.47	1.18	1.21	1.08	1.66
1	1.43	1.12	1.15	1.04	1.51

IV. CONCLUSIONS

The following conclusions are drawn from the preceding discussion of the data collected and processed for three historic through-truss bridges:

- The 95th percentile *DLFs* at each bridge corresponding to normal traffic are higher than the AASHTO specified 1.33, indicating that historic through-truss bridge dynamic response may generally be larger than slab-on-girder bridges. It may be advisable to use a *DLF* of approximately 1.5 for the evaluation of historic through-truss bridges.
- The 95th percentile *DLF* under rating level loading is marginally higher than the AASHTO specified 1.33. This suggests that evaluation of historic through-truss bridges could justify the application of a marginally increased *DLF* of 1.36.
- Normal traffic and test vehicle loading correspond to a positively skewed *DLF* distribution. Comparison of individual bridge *DLF* distributions indicates that as sample size increases, the 95th percentile decreases. Comparison of primary member *DLF* distributions indicates that as static strain level increases, the 95th percentile *DLF* magnitude decreases.
- *DLF* magnitude is most strongly associated with member maximum static stress with a Pearson's correlation coefficient of -0.367 for normal traffic conditions and -0.496 for test vehicle loading.
- High magnitudes of *DLF* correspond with low GVW/low strains and low magnitudes of *DLF* correspond to high GVW/high strains.
- *DLF* magnitude has a negligible relationship to bridge length.
- *DLF* magnitude does not appear to be dependent on truss type. Two truss types were tested. The two tested bridges of similar geometry responded with very different *DLF* distributions.
- It appears that bridge mass and stiffness, which may be related to truss type, are more responsible for changes in *DLF* magnitude than bridge length.
- Vehicle speed is very weakly related to *DLF* magnitude as certain mid-ranges of speed resulted in higher *DLF* magnitudes.

These conclusions can be applied to the dynamic evaluation of historic through-truss bridges. The recommended *DLF*s are also applicable to the design of rehabilitation and replacement of members.

REFERENCES

[1]. American Association of State and Highway Transportation Officials. (1994). AASHTO LRFD Bridge Design Specification. Washington, D.C.

[2]. Ashebo, D. B., Chan, T. H., & Yu, L. (2007). Evaluation of dynamic loads on a skew box girder contiuous bridge Part I: Field test and modal analysis. Engineering Structures (29), 1052-1063.

[3]. Ashebo, D. B., Chan, T. H., & Yu, L. (2007). Evaluation of dynamic loads on a skew box girder contiuous bridge Part II: Parametric study and dynamic load factor. Engineering Structures (29), 1064-1073.

[4]. Billing, J. (1984). Dynamic loading and testing of bridges in Ontario. Canadian Journal of Civil Engineering , 11, 833-843.

[5]. Deng, L., &Cai, C. S. (2010). Development of dynamic impact factor for performance evaluation of existing multi-girder concrete bridges. Engineering Structures (32), 21-31.

[6]. Hwang, E.-S., & Nowak, A. S. (1991). Simulation of Dynamic Load for Bridges. Journal of Structural Engineering , 117 (5), 1413-1434.

[7]. Japan Road Association, Specifications for Highway Bridges, 2014.

[8]. Kim, S., & Nowak, A. S. (1997, August). Load Distribution and Impact Factors for I-Girder Bridges. Journal of Bridge Engineering , 97-104.

[9]. Laman, J. A., Pechar, J. S., & Boothby, T. E. (1999, November). Dynamic Load Allowance for Through-Truss Bridges. Journal of Bridge Engineering , 231-241.

[10]. Merriman, M., & Jacoby, H. S. (1909). A Text-Book on Roofs and Bridges Part III. New York, New York: John Wiley & Sons.

[11]. Moghimi, H., &Ronagh, H. R. (2008). Impact factors for a composite steel bridge using non-linear dynamic simulation. International Journal of Impact Engineering (35), 1228-1243.

[12]. Nowak, A. S., &Szerszen, M. M. (1998). Bridge load and resistance models. EnineeringStructures , 985-990.

[13]. OBrien, E. J., Rattigan, P., Gonzalez, A., Dowling, J., &Znidaric, A. (2009). Characteristic dynamic traffic load effects in bridges. Engineering Structures (31), 1607-1612.

[14]. OConnor, C. M., & Pritchard, R. W. (1985). Impact Studies on Small Composite Girder Bridge. Journal of Structural Engineering , 111 (3), 641-653.

[15]. Paultre, P., Chaallal, O., &Proulx, J. (1992). Bridge dynamics and dynamic amplification factors - a review of analytical and experimental findings. Canadian Journal of Civil Engineering , 260-278.

[16]. Pechar, J. S. (1997). Dynamic Load Factors for Through-Truss Bridges. Masters Thesis, The Pennsylvania State University, Department of Civil and Environmental Engineering.

*Brandon Newpher. "Dynamic Response of Three Historic Through-Truss Bridges." Quest Journals Journal of Architecture and Civil Engineering, vol. 05, no. 09, 2017, pp. 01-11.